Journal of General Virology (2009), **90**, 2695–2703 DOI 10.1099/vir.0.013490-0

Angiotensin-converting enzyme 2 (ACE2) from raccoon dog can serve as an efficient receptor for the spike protein of severe acute respiratory syndrome coronavirus

Lili Xu,[1] Yanfang Zhang,[1] Yun Liu,[1] Zhiwei Chen,[2] Hongkui Deng,[3] Zhongbin Ma,[1] Hualin Wang,[1] Zhihong Hu[1] and Fei Deng[1]

Correspondence
Fei Deng
df@wh.iov.cn

[1]State Key Laboratory of Virology, Wuhan Institute of Virology, Chinese Academy of Sciences, Wuhan 430071, PR China

[2]AIDS Institute, The University of Hong Kong Li Ka Shing Faculty of Medicine, Hong Kong SAR

[3]Department of Cell Biology and Genetics, College of Life Sciences, Peking University, Beijing 100871, PR China

Raccoon dog is one of the suspected intermediate hosts of severe acute respiratory syndrome coronavirus (SARS-CoV). In this study, the angiotensin-converting enzyme 2 (ACE2) gene of raccoon dog (rdACE2) was cloned and sequenced. The amino acid sequence of rdACE2 has identities of 99.3, 89.2, 83.9 and 80.4 % to ACE2 proteins from dog, masked palm civet (pcACE2), human (huACE2) and bat, respectively. There are six amino acid changes in rdACE2 compared with huACE2, and four changes compared with pcACE2, within the 18 residues of ACE2 known to make direct contact with the SARS-CoV S protein. A HeLa cell line stably expressing rdACE2 was established; Western blot analyses and an enzyme-activity assay indicated that the cell line expressed ACE2 at a similar level to two previously established cell lines that express ACE2 from human and masked palm civet, respectively. Human immunodeficiency virus-backboned pseudoviruses expressing spike proteins derived from human SARS-CoV or SARS-CoV-like viruses of masked palm civets and raccoon dogs were tested for their entry efficiency into these cell lines. The results showed that rdACE2 is a more efficient receptor for human SARS-CoV, but not for SARS-CoV-like viruses of masked palm civets and raccoon dogs, than huACE2 or pcACE2. This study provides useful data to elucidate the role of raccoon dog in SARS outbreaks.

Received 20 May 2009
Accepted 19 July 2009

INTRODUCTION

Severe acute respiratory syndrome (SARS), a disease that first occurred in November 2002 in Guangdong Province, China, has caused over 8000 infections worldwide with a fatality rate up to 10 % within several months (WHO, 2004). A novel coronavirus, SARS-CoV, was identified as the aetiological agent of the disease (Drosten *et al.*, 2003; Fouchier *et al.*, 2003; Ksiazek *et al.*, 2003; Peiris *et al.*, 2003) and phylogenetic analysis indicated that the virus was different from previously known coronaviruses (Marra *et al.*, 2003; Rota *et al.*, 2003).

Although the identification of the aetiological agent and molecular studies on SARS-CoV proceeded rather rapidly, the puzzle of the origin of the disease was still not fully resolved. There appears to be a reservoir for SARS-CoV in wild animals, because a high proportion of early SARS patients were food handlers with likely animal contact in Guangdong Province (Normile & Enserink, 2003). SARS-CoV-like viruses with extremely high sequence identity to SARS-CoV were isolated from masked palm civets (*Paguma larvata*) and a raccoon dog (*Nyctereutes procyonoides*) from a live-animal market, suggesting that these animals played important roles in the transmission of SARS-CoV (Guan *et al.*, 2003). Later on, several investigations confirmed that masked palm civet in the market was a critical intermediate host, but not a natural reservoir, for SARS-CoV (Tu *et al.*, 2004; Kan *et al.*, 2005; Poon *et al.*, 2005; Song *et al.*, 2005; Wang *et al.*, 2005). Horseshoe bat was later on identified as a natural reservoir for SARS-CoV-like viruses (Lau *et al.*, 2005; W. Li *et al.*, 2005b); however, the variation of the spike (S) protein of bat SARS-CoV-like virus indicated that the viruses discovered so far from bats cannot infect human cells directly (Ren *et al.*,

The GenBank/EMBL/DDBJ accession number for the full-length sequence of the raccoon dog ACE2 gene determined in this study is EU024940.

2008). Therefore, there are still unknown elements in the transmission cycle of SARS-CoV.

SARS-CoV uses a cell-surface zinc peptidase, angiotensin-converting enzyme 2 (ACE2), as its receptor (Li *et al.*, 2003). ACE2 genes from several species have been sequenced and it has been shown that the efficiencies of infection in humans, mice and rats correlate with the ability of the ACE2 from each species to support virus replication (Li *et al.*, 2004; Subbarao *et al.*, 2004; Wentworth *et al.*, 2004).

Although SARS-CoV-like viruses were detected from raccoon dogs in both 2003 and 2004 (Guan *et al.*, 2003; Kan *et al.*, 2005), very limited research was focused on the role of raccoon dogs in the SARS epidemic. In this study, ACE2 was extracted from raccoon dog, and a HeLa cell line stably expressing the raccoon dog ACE2 (rdACE2) protein was established. By using pseudotyped SARS-CoV, we determined whether rdACE2 can be used as the receptor for SARS-CoV and its efficiency in comparison to ACE2 proteins from human and masked palm civet. We hope that the results further our understanding of the role of the raccoon dog in the SARS epidemic, and provide useful data for prevention of the possible re-emergence of SARS.

METHODS

RNA extraction, DNA sequencing and analysis. RNA was extracted from a mixture of the heart, liver, spleen and lung from a raccoon dog (obtained in October 2006 from a live-animal retail market in Hebei Province, China) with TRIzol (Invitrogen), according to the manufacturer's instructions. RNA was dissolved in 20 μl diethyl pyrocarbonate-treated water and stored at −80 °C.

RNA was reverse-transcribed to cDNA by using a combined gene-specific priming, random-priming and oligo-dT-priming strategy by using SuperScript II reverse transcriptase (Invitrogen). Five overlapping DNA fragments covering the full-length ACE2 gene were produced by PCR using the following primers, which were designed based on the most conserved regions of a sequence alignment of ACE2 genes from ten SARS-associated animals: ACE2F1, 5′-CCGGATCCATGTCAGGCTCTTCCTGGCTC-3′; ACE2F2, 5′-CCGGATCCCTCCTTCAACTTCTTTGTCAC-3′; ACE2F3, 5′-GCGGGATCCCAAGAACCAACGATTGAACAC-3′; ACE2F4, 5′-GCGGGATCCGGTAGATTTTGGACAAATCTGT-3′; ACE2F5, 5′-GCGGGATCCTGGTGGGAGATGAAGCGA-3′; ACE2R1, 5′-GGCTCGAGCTAAATGAAGTCTGAGCATC-3′; ACE2R2, 5′-GGCTCGAGACAAGCTTTTCCAGTACTGTA-3′; ACE2R3, 5′-GCGCTCGAGGTAACATCTATGTTTGGTTTCTG-3′; ACE2R4, 5′-GCGCTCGAGATGTTTCATCATGGGGCACAG-3′; ACE2R5, 5′-GCGCTCGAGACATCCTGATGGCCTCTTC-3′. The underlined sequences are restriction-enzyme digestion sites.

The PCR products were purified and cloned into the pGEM-T Easy vector (Promega) separately for sequencing, which was performed on a CEQ8000 sequencer (Beckman Coulter) with M13 forward and reverse primers (M13F, 5′-CGCCAGGGTTTTCCCAGTCACGAC-3′; M13R, 5′-TCACACAGGAAACAGCTATGAC-3′). Then, all five PCR fragments were spliced by the overlap-extension PCR method (Horton *et al.*, 1989) to obtain the full-length rdACE2 gene, which was sequenced again for absolute accuracy of the rdACE2 sequence.

Alignment analyses of nucleic acid and amino acid sequences were performed by using the CLUSTAL W (version 1.83) software (Thompson *et al.*, 1994). Phylogenetic trees were constructed based on amino acid sequences by using the neighbour-joining algorithm in the MEGA3.1 software package (Kumar *et al.*, 2004).

Generation of cell lines stably expressing ACE2 proteins. The HeLa-huACE2 and HeLa-pcACE2 cell lines, which stably express ACE2 from human and palm civet, respectively, were constructed previously (Qu *et al.*, 2005). Generation of a cell line stably expressing rdACE2 was established by using a Moloney murine leukemia virus-based pseudotyped system termed pVPack (Stratagene). Briefly, the rdACE2 gene was cloned into retroviral vector pFB-Neo to generate pFB-rdACE2, then HEK293T cells were cotransfected by the calcium phosphate method with pFB-rdACE2, a vesicular stomatitis virus protein G (VSV-G)-expressing vector (pVPack-VSV-G) and a *gag–pol*-expressing vector (pVPack-GP). At 48 h post-transfection, viral supernatants were harvested, cell debris was cleared by centrifugation and HeLa cells were then transduced. The medium was replaced 8 h post-transduction and the cells were selected in growth medium containing 800 μg G418 ml^{-1} (Amresco). A cell line stably expressing rdACE2 was selected by limiting dilution for four passages in 1 month.

Rabbit polyclonal antibodies against huACE2, pcACE2 and rdACE2 were generated with recombinant full-length ACE2 proteins expressed in the pProEXHT (Gibco-BRL) expression system. Purified proteins (200 μg) were used to immunize rabbits. After 3 weeks, the rabbits received a booster with the same amount of the antigens. Two weeks later, antisera were collected and stored at −80 °C.

Stable expression of human, palm civet and raccoon dog ACE2 in HeLa cells was detected by using rabbit antibodies against huACE2, pcACE2 and rdACE2, respectively. Also, cross-reactions between ACE2 proteins and anti-ACE2 antibodies were tested. Cell lysates were separated by SDS-PAGE and then transferred to nitrocellulose membranes (Millipore). The membranes were incubated separately with rabbit anti-huACE2, anti-pcACE2 and anti-rdACE2 (1 : 1000) and bound antibodies were detected by using alkaline phosphatase-conjugated goat anti-rabbit IgG (1 : 2000) (SABC). The signal was detected with a BCIP–nitro blue tetrazolium kit (SABC).

Fluorescence-activated cell sorting (FACS) analysis of ACE2-expressing cells. Firstly, rabbit anti-huACE2 antibody was purified by protein A–Sepharose chromatography (Calbiochem) and conjugated with fluorescein isothiocyanate (FITC; AnaSpec) in DMSO (Sigma). Secondly, ACE2-expressing and control HeLa cells were cultured on coverslips in 24-well plates (Corning). The following day, the cells were washed with cold PBS and harvested with PBS containing 5 mM EDTA for 10 min at 4 °C and spun at 1000 ***g*** for 5 min, followed by overnight incubation with FITC-conjugated rabbit anti-huACE2 antibody (at a 1 : 100 dilution in PBS with 3 % goat serum) at 4 °C. The next day, after two washes with cold PBS, the cells were fixed by resuspending them in 2 % paraformaldehyde and incubated at room temperature for 15 min. Finally, the cells were washed twice and resuspended in 500 μl cold PBS, and flow-cytometry analysis (Epics Altra II; Beckman Coulter) was performed.

ACE2 activity assay. The cell-membrane fraction was prepared by using a ProteoPrep Membrane Extraction kit (Sigma). The protein content of the membrane was determined with a BCA Protein Assay kit (Biyotime), using bovine serum albumin as a standard. The activity of the ACE2 assay was determined as described by Douglas *et al.* (2004) using the ACE2-specific quenched fluorescent substrate QFS (7-methoxycoumarin-4-yl)-acetyl-Ala-Pro-Lys(2,4-dinitrophenyl) (Auspep). Assays were performed in black 96-well plates with 50 μM QFS per reaction and incubated at 37 °C for 1 h. Liberated fluorescence (in relative fluorescence units) was measured at

320–420 nm. To demonstrate specific inhibition, ACE2 activity was also determined in the presence of 0.1 mM EDTA.

Construction of full-length S genes with distinct receptor-binding domain (RBD) sequences. Four full-length SARS-CoV S genes with a codon-optimized S backbone from human SARS-CoV, but with distinct RBD sequences from strain BJ01 (human), palm civets in Guangdong Province (pcGD) and in Hubei Province (pcES) and a raccoon dog in Shenzhen from 2003 (rd03SZ), were generated in a previous study (Liu *et al.*, 2007). For the current study, the RBD sequence of the S gene from a raccoon dog in Guangzhou from 2004 (rd04GZ) was constructed by site-directed mutagenesis. Primers were designed based on the sequences of S genes A030 (GenBank accession no. AY687357) and A031 (accession no. AY687358), which were detected in market raccoon dogs in 2004 and have 100 % sequence identity. All five S genes were cloned individually into the pcDNA3.1 vector (Invitrogen). Amino acid differences in the RBDs of the above S glycoproteins are listed in Table 1.

Virus entry assay with HIV-luc/SARS-pseudotyped virus. The pseudoviruses were generated by cotransfecting 5×10^7 HEK293T cells in 100 mm cell-culture dishes (Corning) with a human immunodeficiency virus type 1 (HIV-1) pNL4.3Luc$^+$Env$^-$Vpr$^-$ backbone (30 μg) and one of the above-mentioned, full-length S gene-expression plasmids (30 μg) by using Lipofectamine 2000 (Invitrogen). Viral supernatants were harvested 48 h post-transfection, clarified from cell debris by centrifugation at 3000 ***g*** for 10 min and filtered through a 0.45 μm pore-size filter (Millipore). Pseudoviruses in the cell supernatants were purified by ultracentrifugation through a 20 % sucrose cushion at 55 000 ***g*** for 90 min using a Ty90 rotor (Beckman). The pelleted pseudoviruses were dissolved in 60 μl PBS. To evaluate the incorporation of S proteins and HIV P24 into the pseudotyped viruses, 10 μl of each purified virus was subjected to SDS-PAGE and Western blotting with each antibody. The supernatant was assayed for P24 by using an HIV-1 P24 antigen ELISA kit (provided by the mAb laboratory of the Wuhan Institute of Virology, Chinese Academy of Sciences). HeLa cells (1×10^6 cells) stably expressing similar amounts of huACE2, rdACE2 or pcACE2 were seeded into 24-well plates and transduced 24 h later with equivalent amounts of the respective pseudovirus. The efficiency of virus entry was monitored by a luciferase reporter gene in the pseudovirus (Promega) by using a Turner Designs TD-20/20 luminometer. Each transduction experiment was conducted in triplicate and all experiments were repeated four times.

Statistical analysis. Statistical analysis of the entry efficiencies was performed by SPSS 11.5 software and the DUNCAN and LSD methods were used for detection in one-way ANOVA means.

Table 1. Amino acid differences in the RBDs of S glycoproteins used in this study

Virus	Residue at position						
	344	360	462	472	479	480	487
Human SARS-CoV	K	F	P	L	N	D	T
pcGD	R	S	P	P	N	G	S
pcES	R	F	P	P	R	G	S
rd03SZ	R	S	P	L	K	D	S
rd04GZ	R	S	S	P	R	G	S

RESULTS

Sequence analysis of the rdACE2 protein

The full-length sequence of raccoon dog ACE2 was obtained by cloning and sequencing as described in Methods. The coding region was deposited in GenBank under accession number EU024940.

The rdACE2 gene encodes an 804 aa protein, which is identical in size to the ACE2 protein of dog, but 1 aa shorter than those of human and palm civet. Sequence alignment indicated that the rdACE2 molecule has an amino acid sequence identity of 99.3 % to dog ACE2, 90.7 % to cat ACE2, 90.5 % to raccoon ACE2, 89.2 % to pcACE2, 83.9 % to huACE2, 81.6 % to mouse ACE2, 81.4 % to rat ACE2, 80.5 % to ferret ACE2 and 80.4 % to bat ACE2. ACE2 of raccoon dog was almost identical to dog ACE2, with only six amino acid differences at residues 26, 52, 59, 326, 340 and 353. A sequence alignment and a phylogenetic tree are shown in Fig. 1. There appear to be four groups of ACE2 proteins based on phylogenetic analysis: group I contains the ACE2 proteins of raccoon dog, dog, ferret, raccoon, masked palm civet and cat, group II contains those of human and VeroE6 cells, group III contains those of mouse and rat and group IV contains that of bat (Fig. 1b).

It was reported that there are 18 residues of ACE2 that make direct contact with the SARS-CoV S protein (F. Li *et al.*, 2005) (Table 2, columns marked *). For these 18 residues, there are six changes in rdACE2 compared with the cognate human protein: Q24L (Q in huACE2 and L in rdACE2 at residue 24), H34Y, D38E, M82T, N90D and K353R, and four changes compared with pcACE2 (T31K, Q37E, V45L and K353R). Three regions within the S–ACE2 complex domain (W. Li *et al.*, 2005a) differed significantly between rdACE2, huACE2 and pcACE2 (Table 2): the region of α-helix 1 (residues 30–41) varied at four residues from huACE2 and two from pcACE2; the loop initiating ACE2 α-helix 3 (residues 90–93) differed by two residues from huACE2 and three from pcACE2; and a loop and β5 (residues 353–357) had only one variation in rdACE2, and this variation (K353R in rdACE2) has never been found in any other species (although there is a histidine in the mouse and rat ACE2 proteins). This position was reported to be one of the most critical residues in ACE2 for binding to the SARS-CoV S protein (Li, 2008; F. Li *et al.*, 2005; W. Li *et al.*, 2005a).

Generation of a HeLa cell line stably expressing the rdACE2 protein

A HeLa cell line that stably expresses the rdACE2 protein was established as described in Methods. Rabbit polyclonal antibodies against huACE2, pcACE2 and rdACE2 were generated by using recombinant prokaryotic-expressed full-length ACE2 proteins. Western blot analysis showed that rdACE2 was expressed efficiently in HeLa cells and was

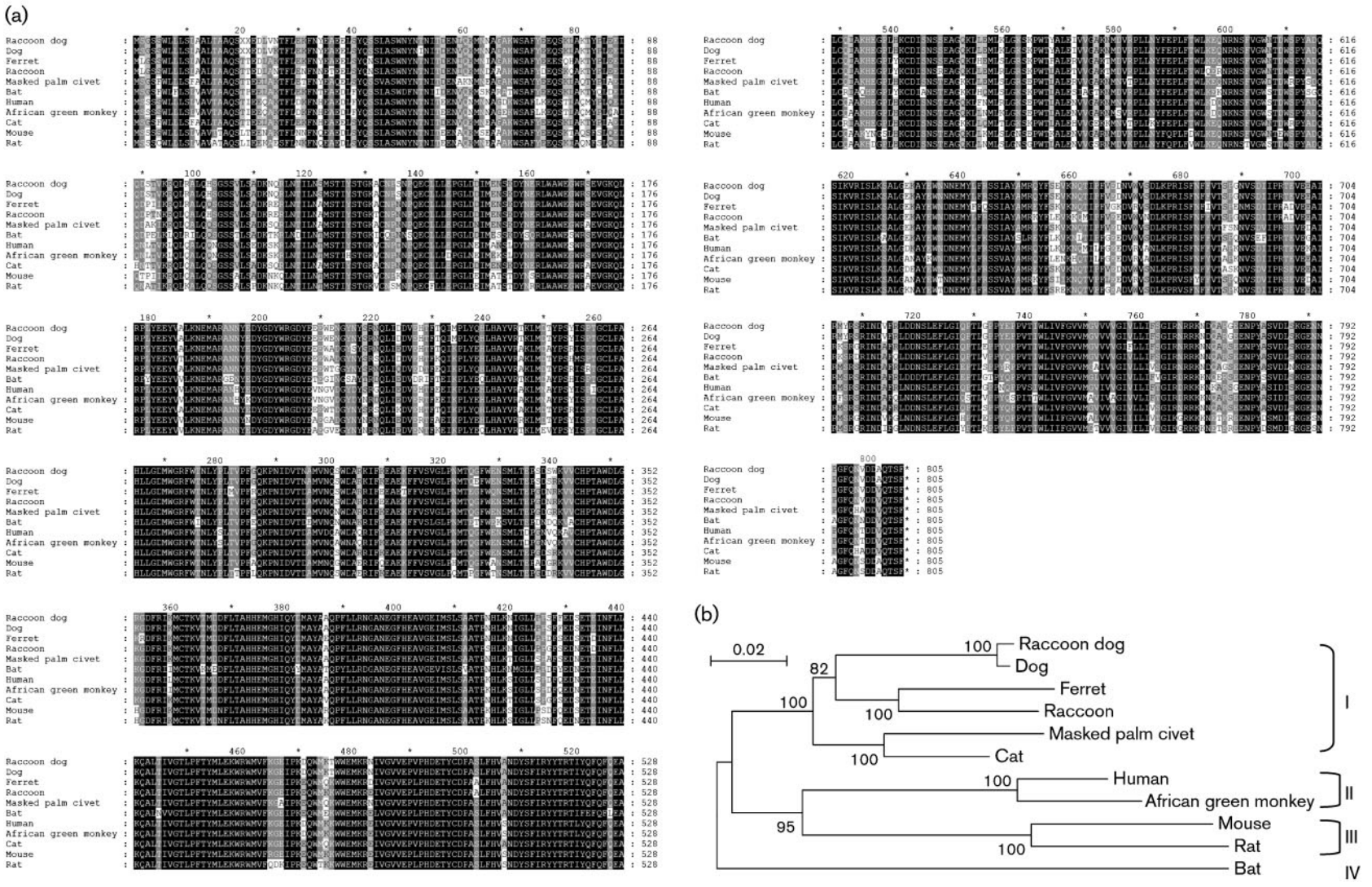

Fig. 1. Sequence analysis of rdACE2. (a) Multiple amino acid sequence alignment of ACE2 from different mammals. The GenBank accession numbers for the ACE2 proteins are as follows: raccoon dog, EU024940; dog, XM_537964; ferret, AB208708; raccoon, AB211998; masked palm civet, AY881174; bat, AB299376; human, AB193260.1; African green monkey, AY996037; cat, AB211997; mouse, AK141604; rat, AY881244. (b) A phylogenetic tree was constructed based on amino acid sequences of different ACE2 proteins using the neighbour-joining algorithm in the MEGA3.1 software package, with bootstrap values (%) determined by 500 replicates.

Table 2. Contacts between ACE2 and SARS-CoV RBD

Residues in ACE2 that have contact with the RBD are listed by their position and single-letter identity. Non-identical residues are shown in bold type. The residues in the S protein from human isolates that contact ACE2 are shown at the bottom of each column.

ACE2 protein	24*	27*	30	31*	32	33	34*	35	36	37*	38*	39	40	41*	42*	45*	79*	82*	83*	90*	91	92	93	325*	329*	330*	353*	354*	355	356	357
Raccoon dog	L	T	E	K	F	N	**Y**	E	A	E	E	L	S	Y	Q	L	L	T	Y	D	**S**	T	**V**	Q	E	N	**R**	G	D	F	R
Dog	L	T	E	K	F	N	**Y**	E	A	E	E	L	S	Y	Q	L	L	T	Y	D	**S**	T	**V**	Q	E	N	K	G	D	F	R
Ferret	L	T	E	K	F	N	**Y**	E	A	E	E	L	S	Y	Q	L	**H**	T	Y	D	P	**I**	I	**E**	**Q**	N	K	**R**	D	F	R
Raccoon	L	T	E	**N**	F	N	**N**	E	**T**	E	E	L	S	Y	Q	L	**Q**	T	Y	D	P	T	**N**	Q	E	N	K	G	D	F	R
Palm civet	L	T	E	**T**	F	N	**Y**	E	A	**Q**	E	L	S	Y	Q	**V**	L	T	Y	D	**A**	**K**	I	Q	E	N	K	G	D	F	R
Bat	L	T	E	K	F	N	**T**	E	A	E	**D**	L	**F**	Y	Q	L	L	T	Y	D	P	**E**	**L**	**E**	E	**K**	K	G	D	F	R
Human	**Q**	T	**D**	K	F	N	**H**	E	A	E	**D**	L	**F**	Y	Q	L	L	**M**	Y	**N**	**L**	T	**V**	Q	E	N	K	G	D	F	R
Mouse	**N**	T	**N**	**N**	F	N	**Q**	E	A	E	**D**	L	S	Y	Q	L	**T**	**S**	**F**	**T**	P	**I**	I	Q	**A**	N	**H**	G	D	F	R
Rat	**K**	**S**	**N**	K	F	N	**Q**	E	A	E	**D**	L	S	Y	Q	L	**I**	**N**	**F**	D	**A**	T	I	**P**	**T**	N	**H**	G	D	F	R
Human	N473	Y475		Y475,			Y440,			Y491	Y436			Y484,	Y436,	Y484	L472	L472	N473,	T402				R426	R426	T486	G488,	Y491,			
SARS-CoV S				Y442			N479							T486,	Y484				Y475								T487,	G488			
														T487													Y491				

*These columns denote the 18 residues of ACE2 known to make direct contact with the SARS-CoV S protein.

recognized by anti-rdACE2 antibody (Fig. 2). Moreover, cross-reactions with the three antibodies indicated that the cell lines expressed comparable amounts of the different proteins and that any of the antisera can be used effectively to detect the receptors from the three species (Fig. 2).

To detect the expression of ACE2 at the cell surface, FACS analysis was performed. The result is shown in Fig. 3. Cells stably expressing huACE2, pcACE2 or rdACE2 exhibited comparable positive-cell ratios ($P>0.05$) when using FITC-conjugated rabbit anti-huACE2 antibody for detection, which were significantly higher than those for the control HeLa cells.

ACE2 proteins were assessed further by an enzyme-activity assay using an ACE2-specific peptide substrate, QFS. As shown in Fig. 4, membrane fractions prepared from the three cell lines displayed substantially higher protease activities toward QFS than the control HeLa cells (Fig. 4a). Furthermore, the protease activity was largely abolished in the presence of 0.1 mM EDTA, a known inhibitor of ACE2 proteases (Fig. 4b).

Analysis of S protein expression and pseudovirus packaging

The expression of different S proteins and their correct incorporation into pseudoviruses were monitored by Western blotting of purified virions using both S- and P24-specific mAbs. Pseudoviruses were purified by ultra-centrifugation through a 20 % sucrose cushion and subjected to SDS-PAGE for Western blotting with each antibody. The results showed that all genes encoding an S protein were expressed efficiently and incorporated into the respective pseudoviruses at comparable levels (Fig. 5).

Comparison of the entry efficiencies of different pseudoviruses into different ACE2-expressing cells

As shown in Fig. 6, when HIV/human-S pseudovirus was used to infect HeLa-huACE2, HeLa-pcACE2 and HeLa-rdACE2 cells, higher levels of luciferase activity ($>2\times10^5$ relative light units) were detected in the cell lysates of HeLa-rdACE2 than in HeLa-huACE2 and HeLa-pcACE2 cell lysates. If the entry efficiency of HIV/human-S pseudovirus into HeLa-rdACE2 cells was defined as 100 %, then those of HIV/human-S pseudovirus into HeLa-huACE2 and HeLa-pcACE2 cells were 65.6 and 53.0 %, respectively. Statistical analysis by SPSS software indicated that the entry efficiencies were significantly different from each other when HIV/human-S pseudovirus infected the three ACE2-expressing cell lines ($P<0.01$). In contrast, when other animal-derived pseudoviruses were used to infect HeLa-rdACE2 cells, much lower luciferase activities were observed, especially when raccoon dog-derived pseudoviruses (HIV/rd03SZ-S and HIV/rd04GZ-S) were used. In the latter case, approximately 10^3 relative light units were detected, and the infection abilities were

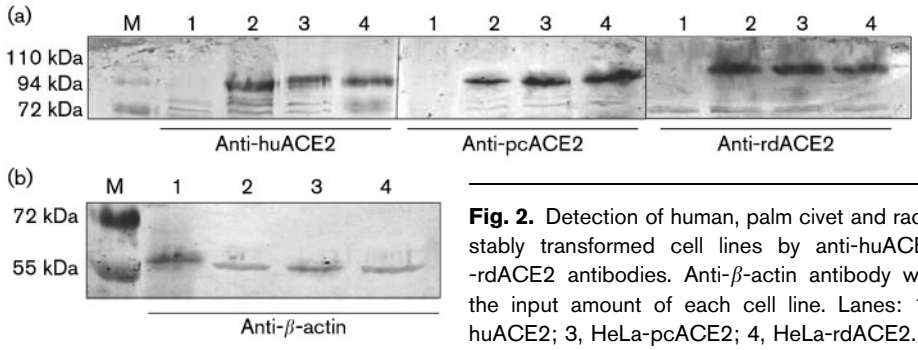

Fig. 2. Detection of human, palm civet and raccoon dog ACE2 in stably transformed cell lines by anti-huACE2, -pcACE2 and -rdACE2 antibodies. Anti-β-actin antibody was used to detect the input amount of each cell line. Lanes: 1, HeLa; 2, HeLa-huACE2; 3, HeLa-pcACE2; 4, HeLa-rdACE2.

<3 % (1.5 and 2.5 %, respectively) of that of HIV/human-S pseudovirus infected into HeLa-rdACE2 cells. Statistical analyses showed that, when HeLa-huACE2 and HeLa-rdACE2 cells were infected by HIV/rd03SZ-S and HIV/rd04GZ-S, the difference in entry efficiencies is not significant ($P>0.05$). However, it seems that HeLa-pcACE2 is relatively more acceptable to both HIV/rd03SZ-S and HIV/rd04GZ-S than HeLa-huACE2 and HeLa-rdACE2 ($P<0.01$). Meanwhile, we also observed that huACE2 is most sensitive to human-derived SARS-CoV, and pcACE2 is most sensitive to masked palm civet-derived SARS-CoV-like viruses, consistent with previous reports (W. Li *et al.*, 2005a; Liu *et al.*, 2007).

DISCUSSION

In this study, ACE2 from raccoon dog was cloned, sequenced and compared with ACE2s from human and palm civet for entry efficiency of SARS-CoV and SARS-CoV-like viruses.

Our results showed that rdACE2 could mediate human SARS-CoV entry more efficiently than huACE2 and pcACE2. Sequence analysis revealed that there are six changes in rdACE2 compared with huACE2, and four changes compared with pcACE2, within the 18 residues of ACE2 known to make direct contact with the SARS-CoV S protein (F. Li *et al.*, 2005) (Table 2). These changes may contribute to the increased entry efficiency of human SARS-CoV. The most noticeable residue was 353, which was an arginine in rdACE2 that has never been found in any other species (although a histidine has been reported at this position in mouse and rat ACE2 proteins). This position was reported to be one of the most critical residues in ACE2 for binding the SARS-CoV S protein (F. Li *et al.*, 2005; W. Li *et al.*, 2005a; Li, 2008). W. Li *et al.* (2005a) made a series of huACE2 variants in which one or a few solvent-exposed residues were altered to their rat ACE2 counterparts. Alteration of lysine 353 to a histidine residue, as present on the rat receptor, dramatically inhibited S protein-mediated entry. In contrast, introduction of human lysine 353 into rat ACE2 converted it to an efficient receptor for SARS-CoV. These data suggested that residue 353 in ACE2 plays a critical role in S-protein binding and subsequent cell entry. Structural studies of huACE2 complexed with the human SARS-CoV S-protein RBD suggested that the side chain of ACE2 Lys353 folds back and is embedded in a hydrophobic tunnel surrounded by Tyr484, Tyr491 and Thr487 of the RBD and Tyr41 of ACE2. At the opening of the tunnel is Asp38 of ACE2, which neutralizes the charge of Lys353 and stabilizes the interface. The stability and intensity of this complex appear to be critical for S–ACE2 interaction activity (F. Li *et al.*, 2005; Li, 2008). On rdACE2, Arg353 is present instead of Lys353 (which is present in the human and palm civet ACE2 proteins). Both arginine and lysine are positive-charged amino acids and arginine has a longer side chain, which may embed more deeply and more stably into the hydrophobic tunnel surrounded by residues 484, 491 and 487 of the RBD and residue 41 of ACE2. Interestingly, Glu38 occurs in rdACE2 instead of Asp38 in huACE2, both of which are negative-charged amino acids that can neutralize the positive charge of residue 353 and stabilize the interface. It is plausible that, in comparison to the human and palm civet ACE2 proteins, residue 353 of rdACE2 interacts more stably with surrounding residues and, with the interaction of Glu38, results in a more efficient SARS-CoV S-binding activity.

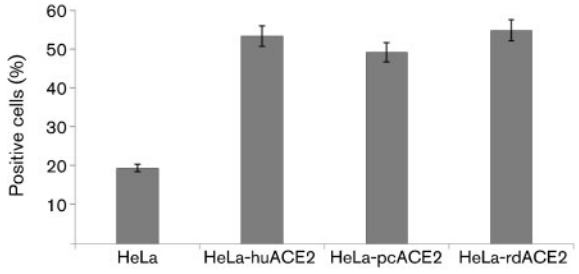

Fig. 3. FACS analysis of ACE2-expressing HeLa cell lines. HeLa cells with no exogenous ACE2 gene were used as negative controls. HeLa cells expressing huACE2, pcACE2 and rdACE2 were detected by FACS using FITC-conjugated rabbit anti-huACE2 antibody. Error bars indicate SD.

It is then interesting to know why, when pseudoviruses derived from palm civets and raccoon dogs were used, the binding efficiencies with rdACE2 were not higher than

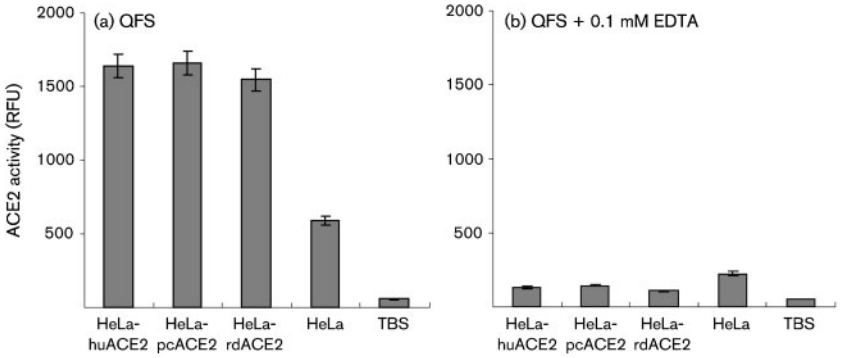

Fig. 4. Determination of ACE2 activity. Protease activities from different ACE2-expressing cell-membrane fractions were determined by using the ACE2-specific substrate QFS (see Methods). Liberated fluorescence [in relative fluorescence units (RFU)] determined at 320–420 nm in the absence (a) and presence (b) of EDTA is shown. HeLa cells with no exogenous ACE2 gene and TBS buffer were used as negative controls. Error bars indicate SD.

those of huACE2 and pcACE2. Li (2008) reported that the side chain of residue 38 of ACE2 by itself was not sufficient to form a strong and stable salt-bridge bond with residue 353, which appears to require support from the γ-methyl group of RBD Thr487. The γ-methyl group of the side chain of RBD Thr487 is important for placing the side chain of ACE2 residue 353 in position to form a salt bridge with ACE2 residue 38. Without this methyl group, residues at position 353 would not be able to form a strong and stable salt bridge with residue 38, leaving a free positive charge in a hydrophobic tunnel and destabilizing the interface (Li, 2008). However, RBD Thr487 in the human S protein is replaced by Ser487 in the palm civet and raccoon dog S proteins, and there is no γ-methyl group in Ser487. It has also been reported that Ser487 on RBD dramatically reduces the affinity for huACE2 by over 20-fold (W. Li *et al.*, 2005a; Qu *et al.*, 2005). This may explain why pseudoviruses derived from SARS-CoV-like viruses of palm civets and raccoon dogs had lower entry efficiencies into HeLa-rdACE2 cells than human SARS-CoV.

Another phenomenon that we observed in this study was that HeLa-pcACE2 cells are relatively more sensitive to pseudoviruses derived from SARS-CoV-like viruses of palm civets and raccoon dogs than HeLa-huACE2 and HeLa-rdACE2 cells, consistent with previous reports that pcACE2 was comparatively more susceptible to different S proteins than huACE2 (W. Li *et al.*, 2005a; Li *et al.*, 2006; Li, 2008). Meanwhile, we also observed that huACE2 is most sensitive to human-derived SARS-CoV, and palm civet-derived SARS-CoV-like viruses are most infectious to pcACE2, which has been reported previously (W. Li *et al.*, 2005a; Liu *et al.*, 2007).

In our study, the entry efficiency of pesudoviruses derived from raccoon dog S proteins was poor in the cell lines expressing huACE2, pcACE2 or rdACE2. This may reflect that the SARS-CoV-like viruses from raccoon dogs could not use these ACE2 proteins efficiently for cell entry. Amino acid sequence alignments of S-protein RBDs showed that rd04GZ has two single-nucleotide polymorphisms (SNPs) compared with pcGD or pcES: residues 462, 479 and 360. However, their infectivities are distinct, which

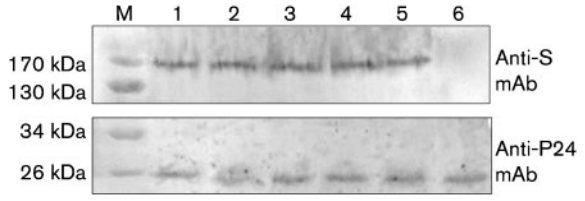

Fig. 5. Detection of S protein incorporated into pseudoviruses. Western blotting of purified virions was performed with S-specific and P24-specific mAbs. Lanes: 1, HIV/human-S; 2, HIV/pcGD S; 3, HIV/pcES S; 4, HIV/rd03SZ S; 5, HIV/rd04GZ S; 6, HIV.

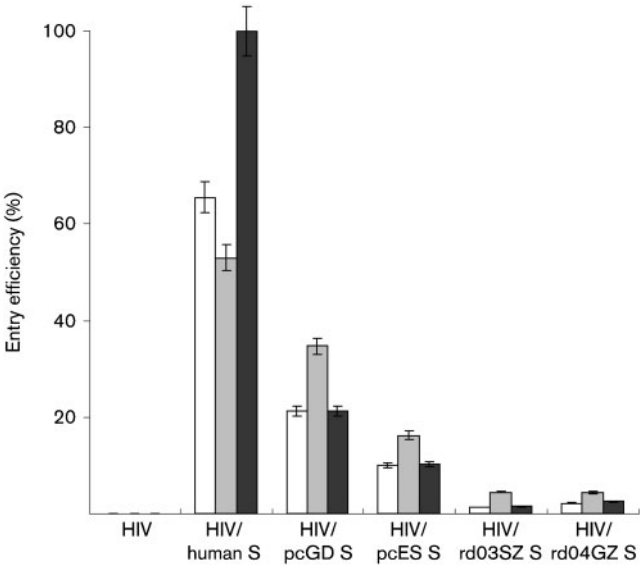

Fig. 6. Comparison of the entry efficiencies of different pseudoviruses into different ACE2-expressing cells. Five pseudoviruses derived from human, palm civet and raccoon dog are shown on the *x*-axis; detected luciferase activity/entry efficiency is shown on the *y*-axis. The entry efficiency of human-derived pseudovirus into HeLa-rdACE2 cells was regarded as 100 %. Empty, shaded and filled bars represent the entry efficiencies of different pseudoviruses into HeLa-huACE2, HeLa-pcACE2 and HeLa-rdACE2 cells, respectively.

means these three residues may have certain impacts on S–ACE2 interaction. Meanwhile, when the two raccoon dog-derived viruses were compared, there are four SNPs in the RBD: residues 462, 472, 479 and 480. Although their infectivities are very similar, it is possible that, when these four SNPs exist together, the influence on S–ACE2 interaction is limited. However, when another two mutations at residues 344 and 487 are added to the above four SNPs, virus entry efficiencies are inhibited dramatically, despite the hypothesis of Qu *et al.* (2005) and Li (2008) that the inhibition was mainly caused by mutations of residues 479 and 487. However, we need to mention that, apart from the RBD region, other parts of the S genes from the raccoon dog viruses also contain mutations that may have impacts on entry efficiency. Therefore, a more desirable conclusion can only be addressed when full-length S genes are used. It is also possible that another unknown molecule in the raccoon dog may serve as a receptor or co-receptor for raccoon dog SARS-CoV-like viruses, which will require further studies for verification.

Notably, amino acid sequence analysis indicated that rdACE2 has an identity of 99.3 % to dog ACE2. Whether dogs are also susceptible to SARS-CoV infection is worthy of study. If so, dogs may be a good candidate for an animal model for SARS-CoV.

In summary, our results suggest that rdACE2 is a more efficient receptor for human SARS-CoV, but not for SARS-CoV-like viruses from palm civets and raccoon dogs, than the human and palm civet ACE2 proteins. The data indicate that raccoon dog may serve as a critical intermediate host for SARS-CoV and may play an important role in SARS outbreaks. The highly efficient interaction between SARS-CoV and rdACE2 may impose an important impact on the evolution of human SARS-CoV, whilst other host and environmental factors may also contribute to the emergence and spread of SARS-CoV. Therefore, further studies are required to understand completely the initiation of SARS outbreaks and animal reservoirs.

ACKNOWLEDGEMENTS

This work was supported by MOST projects (2003CB514118, 2005CB523004 and a special grant for 'Animal Reservoir of SARS-CoV'), and by EU FP6 projects DISSECT (no. SP22-CT-2004-511060) and EPISARS (no. SP22-CT-2004-511603). We thank Dr Basil M. Arif for scientific editing of the manuscript. We also thank Dr Zhengli Shi (Wuhan Institute of Virology, CAS) for providing the pVPack pseudovirus system and Dr Linfa Wang (Australian Animal Health Laboratory, CSIRO) for providing QFS and for helpful discussions.

REFERENCES

Douglas, G. C., O'Bryan, M. K., Hedger, M. P., Lee, D. K., Yarski, M. A., Smith, A. I. & Lew, R. A. (2004). The novel angiotensin-converting enzyme (ACE) homolog, ACE2, is selectively expressed by adult Leydig cells of the testis. *Endocrinology* **145**, 4703–4711.

Drosten, C., Gunther, S., Preiser, W., van der Werf, S., Brodt, H. R., Becker, S., Rabenau, H., Panning, M., Kolesnikova, L. & other authors (2003). Identification of a novel coronavirus in patients with severe acute respiratory syndrome. *N Engl J Med* **348**, 1967–1976.

Fouchier, R. A., Kuiken, T., Schutten, M., van Amerongen, G., van Doornum, G. J., van den Hoogen, B. G., Peiris, M., Lim, W., Stohr, K. & Osterhaus, A. D. (2003). Aetiology: Koch's postulates fulfilled for SARS virus. *Nature* **423**, 240.

Guan, Y., Zheng, B. J., He, Y. Q., Liu, X. L., Zhuang, Z. X., Cheung, C. L., Luo, S. W., Li, P. H., Zhang, L. J. & other authors (2003). Isolation and characterization of viruses related to the SARS coronavirus from animals in southern China. *Science* **302**, 276–278.

Horton, R. M., Hunt, H. D., Ho, S. N., Pullen, J. K. & Pease, L. R. (1989). Engineering hybrid genes without the use of restriction enzymes: gene splicing by overlap extension. *Gene* **77**, 61–68.

Kan, B., Wang, M., Jing, H., Xu, H., Jiang, X., Yan, M., Liang, W., Zheng, H., Wan, K. & other authors (2005). Molecular evolution analysis and geographic investigation of severe acute respiratory syndrome coronavirus-like virus in palm civets at an animal market and on farms. *J Virol* **79**, 11892–11900.

Ksiazek, T. G., Erdman, D., Goldsmith, C. S., Zaki, S. R., Peret, T., Emery, S., Tong, S., Urbani, C., Comer, J. A. & other authors (2003). A novel coronavirus associated with severe acute respiratory syndrome. *N Engl J Med* **348**, 1953–1966.

Kumar, S., Tamura, K. & Nei, M. (2004). MEGA3: integrated software for molecular evolutionary genetics analysis and sequence alignment. *Brief Bioinform* **5**, 150–163.

Lau, S. K., Woo, P. C., Li, K. S., Huang, Y., Tsoi, H. W., Wong, B. H., Wong, S. S., Leung, S. Y., Chan, K. H. & Yuen, K. Y. (2005). Severe acute respiratory syndrome coronavirus-like virus in Chinese horseshoe bats. *Proc Natl Acad Sci U S A* **102**, 14040–14045.

Li, F. (2008). Structural analysis of major species barriers between humans and palm civets for severe acute respiratory syndrome coronavirus infections. *J Virol* **82**, 6984–6991.

Li, W., Moore, M. J., Vasilieva, N., Sui, J., Wong, S. K., Berne, M. A., Somasundaran, M., Sullivan, J. L., Luzuriaga, K. & other authors (2003). Angiotensin-converting enzyme 2 is a functional receptor for the SARS coronavirus. *Nature* **426**, 450–454.

Li, W.,, Greenough, H. T. C., Moore, M. J., Vasilieva, N., Somasundaran, M., Sullivan, J. L., Farzan, M. & Choe, H. (2004). Efficient replication of severe acute respiratory syndrome coronavirus in mouse cells is limited by murine angiotensin-converting enzyme 2. *J Virol* **78**, 11429–11433.

Li, F., Li, W., Farzan, M. & Harrison, S. C. (2005). Structure of SARS coronavirus spike receptor-binding domain complexed with receptor. *Science* **309**, 1864–1868.

Li, W., Zhang, C., Sui, J., Kuhn, J. H., Moore, M. J., Luo, S., Wong, S. K., Huang, I. C., Xu, K. & other authors (2005a). Receptor and viral determinants of SARS-coronavirus adaptation to human ACE2. *EMBO J* **24**, 1634–1643.

Li, W., Shi, Z., Yu, M., Ren, W., Smith, C., Epstein, J. H., Wang, H., Crameri, G., Hu, Z. & other authors (2005b). Bats are natural reservoirs of SARS-like coronaviruses. *Science* **310**, 676–679.

Li, W., Wong, S. K., Li, F., Kuhn, J. H., Huang, I. C., Choe, H. & Farzan, M. (2006). Animal origins of the severe acute respiratory syndrome coronavirus: insight from ACE2-S-protein interactions. *J Virol* **80**, 4211–4219.

Liu, L., Fang, Q., Deng, F., Wang, H. Z., Yi, C. E., Ba, L., Yu, W. J., Lin, R. D., Li, T. S., Hu, Z. H., Ho, D. D., Zhang, L. Q. & Chen, Z. W. (2007). Natural mutations in the receptor binding domain of spike glycoprotein determine the reactivity of cross-neutralization between palm civet coronavirus and severe acute respiratory syndrome coronavirus. *J Virol* **81**, 4694–4700.

Marra, M. A., Jones, S. J., Astell, C. R., Holt, R. A., Brooks-Wilson, A., Butterfield, Y. S., Khattra, J., Asano, J. K., Barber, S. A. & other authors (2003). The genome sequence of the SARS-associated coronavirus. *Science* **300**, 1399–1404.

Normile, D. & Enserink, M. (2003). SARS in China. Tracking the roots of a killer. *Science* **301**, 297–299.

Peiris, J. S., Lai, S. T., Poon, L. L., Guan, Y., Yam, L. Y., Lim, W., Nicholls, J., Yee, W. K., Yan, W. W. & other authors (2003). Coronavirus as a possible cause of severe acute respiratory syndrome. *Lancet* **361**, 1319–1325.

Poon, L. L., Chu, D. K., Chan, K. H., Wong, O. K., Ellis, T. M., Leung, Y. H., Lau, S. K., Woo, P. C., Suen, K. Y. & other authors (2005). Identification of a novel coronavirus in bats. *J Virol* **79**, 2001–2009.

Qu, X. X., Hao, P., Song, X. J., Jiang, S. M., Liu, Y. X., Wang, P. G., Rao, X., Song, H. D., Wang, S. Y. & other authors (2005). Identification of two critical amino acid residues of the severe acute respiratory syndrome coronavirus spike protein for its variation in zoonotic tropism transition via a double substitution strategy. *J Biol Chem* **280**, 29588–29595.

Ren, W., Qu, X., Li, W., Han, Z., Yu, M., Zhou, P., Zhang, S. Y., Wang, L. F., Deng, H. & Shi, Z. (2008). Difference in receptor usage between severe acute respiratory syndrome (SARS) coronavirus and SARS-like coronavirus of bat origin. *J Virol* **82**, 1899–1907.

Rota, P. A., Oberste, M. S., Monroe, S. S., Nix, W. A., Campagnoli, R., Icenogle, J. P., Penaranda, S., Bankamp, B., Maher, K. & other authors (2003). Characterization of a novel coronavirus associated with severe acute respiratory syndrome. *Science* **300**, 1394–1399.

Song, H. D., Tu, C. C., Zhang, G. W., Wang, S. Y., Zheng, K., Lei, L. C., Chen, Q. X., Gao, Y. W., Zhou, H. Q. & other authors (2005). Cross-host evolution of severe acute respiratory syndrome coronavirus in palm civet and human. *Proc Natl Acad Sci U S A* **102**, 2430–2435.

Subbarao, K., McAuliffe, J., Vogel, L., Fahle, G., Fischer, S., Tatti, K., Packard, M., Shieh, W. J., Zaki, S. & Murphy, B. (2004). Prior infection and passive transfer of neutralizing antibody prevent replication of severe acute respiratory syndrome coronavirus in the respiratory tract of mice. *J Virol* **78**, 3572–3577.

Thompson, J. D., Higgins, D. G. & Gibson, T. J. (1994). CLUSTAL W: improving the sensitivity of progressive multiple sequence alignment through sequence weighting, position-specific gap penalties and weight matrix choice. *Nucleic Acids Res* **22**, 4673–4680.

Tu, C., Crameri, G., Kong, X., Chen, J., Sun, Y., Yu, M., Xiang, H., Xia, X., Liu, S. & other authors (2004). Antibodies to SARS coronavirus in civets. *Emerg Infect Dis* **10**, 2244–2248.

Wang, M., Jing, H. Q., Xu, H. F., Jiang, X. G., Kan, B., Liu, Q. Y., Wan, K. L., Cui, B. Y., Zheng, H. & other authors (2005). Surveillance on severe acute respiratory syndrome associated coronavirus in animals at a live animal market of Guangzhou in 2004. *Zhonghua Liu Xing Bing Xue Za Zhi* **26**, 84–87 (in Chinese).

Wentworth, D. E., Gillim-Ross, L., Espina, N. & Bernard, K. A. (2004). Mice susceptible to SARS coronavirus. *Emerg Infect Dis* **10**, 1293–1296.

WHO (2004). Summary of probable SARS cases with onset of illness from 1 November 2002 to 31 July 2003. Accessed 21 April 2004, at http://www.who.int/csr/sars/country/table2004_04_21/en/index.html